

# The crystal structure of paranatrolite

YURI V. SERYOTKIN<sup>1,\*</sup>, VLADIMIR V. BAKAKIN<sup>2</sup> and IGOR A. BELITSKY<sup>1</sup>

<sup>1</sup>Institute of Mineralogy and Petrography, Russian Academy of Sciences, Koptyug prosp. 3, 630090 Novosibirsk, Russia

<sup>2</sup>Institute of Inorganic Chemistry, Russian Academy of Sciences, Lavrentiev prosp 3, 630090 Novosibirsk, Russia

**Abstract:** Paranatrolite from the Khibiny massif, Kola Peninsula, Russia,  $\text{Na}_{1.88}\text{K}_{0.22}\text{Ca}_{0.06}[\text{Al}_{2.24}\text{Si}_{2.76}\text{O}_{10}]\cdot 3.1\text{H}_2\text{O}$ , is monoclinic (space group *Cc*,  $Z = 4$ ). For better comparison of this mineral with the related structure of natrolite, we have selected a pseudo-orthorhombic setting in *F1d1* ( $a = 18.971(4)$ ,  $b = 19.204(3)$ ,  $c = 6.5952(12)$  Å,  $\beta = 91.601(18)^\circ$ ,  $Z = 8$ ). The dominant  $\text{Na}^+$  cations are situated near the sodium positions in the natrolite structure. Additional positions occupied by  $\text{K}^+$  are located in the eight-membered rings.  $\text{H}_2\text{O}$  molecules are located in four independent positions, two being occupied statistically. The Na-polyhedra correspond to distorted  $\text{NaO}_3(\text{H}_2\text{O})_3$  octahedra forming chains along the *c* axis by sharing common  $\text{H}_2\text{O}-\text{H}_2\text{O}$  edges and  $\text{H}_2\text{O}$  vertices. The availability of potassium in the structure results in two configurations for the coordination environment of  $\text{Na}^+$ .

**Key-words:** zeolite, natrolite, paranatrolite, tetranatrolite, crystal structure.

## Introduction

Paranatrolite,  $(\text{Na,K,Ca}_{0.5})_{2+x}[\text{Al}_{2+x}\text{Si}_{3-x}\text{O}_{10}]\cdot 3\text{H}_2\text{O}$ , is a rare and scarcely studied zeolite. It was originally described by Chao (1980) in samples from miarolitic cavities and pegmatitic dykes in nepheline syenites (Mont St-Hilaire, Québec, Canada). Later, Khomyakov *et al.* (1986) discovered and studied this mineral in pegmatites and hydrothermalites from the nepheline syenite massifs of Khibiny and Lovozero (Kola Peninsula, Russia). According to Chao (1980), paranatrolite from Mont St-Hilaire ( $\text{Na}_{1.75}\text{Ca}_{0.10}\text{K}_{0.09}[\text{Fe}_{0.01}\text{Al}_{1.95}\text{Si}_{3.02}\text{O}_{10}]\cdot 2.98\text{H}_2\text{O}$ ) is unstable under dry-air conditions. At low humidity, part of the water is lost and paranatrolite transforms into tetranatrolite. Khomyakov *et al.* (1986) reported a greater stability of paranatrolite from the Khibiny massif,  $\text{Na}_{2.01}\text{K}_{0.22}\text{Ca}_{0.02}[\text{Al}_{2.26}\text{Si}_{2.74}\text{O}_{10}]\cdot 3.1\text{H}_2\text{O}$ , which is able to persist in air for long time. This was associated with a noticeable amount of potassium as a stabilizer in these samples.

Paranatrolite belongs to the structure family of natrolite,  $\text{Na}_2[\text{Al}_2\text{Si}_3\text{O}_{10}]\cdot 2\text{H}_2\text{O}$ , with the same framework topology (NAT). However, the location and coordination of extraframework cations and  $\text{H}_2\text{O}$  molecules has remained uncertain. Literature data on paranatrolite reported the unit-cell parameters obtained from powder diffraction research as well as the proposed crystal system for this mineral (Chao, 1980).

The first structural data on paranatrolite were presented in a paper by Pechar (1988). However, later studies performed by Baur (1991) and our group in Novosibirsk demonstrated clearly that the article of Pechar contains serious errors, so the results have been discredited.

The present paper is concerned with the structure determination of paranatrolite.

It is noteworthy that, in the nomenclature for zeolite minerals recommended by the subcommittee on zeolites of the IMA (Coombs *et al.*, 1997), there is some doubt about the existence of paranatrolite as a separate mineral species. In our opinion, however, the assignment of paranatrolite to overhydrated natrolite, tetranatrolite or gonnardite is incorrect. As reported by Belitsky *et al.* (1992), a further hydration of natrolite is possible only under a water pressure of 7.5 kbar, and the formation of the new phase is reversible. Though gonnardite,  $(\text{Na,Ca})_2[(\text{Al,Si})_5\text{O}_{10}]\cdot 3\text{H}_2\text{O}$ , shows a close relationship with paranatrolite concerning the amount of water in the structure, it has a different paragenesis, according to Evans *et al.* (2000). Thus, these species cannot be considered as related genetically. Moreover, gonnardite differs from paranatrolite in its stability against dehydration under atmospheric conditions. As for a comparison between para- and tetranatrolite, we agree with other researchers that tetranatrolite forms upon paranatrolite dehydration only and thus can be considered as its derivative.

\*E-mail: yuvs@uiggm.nsc.ru

Table 1. Crystal and experimental data of the paranatrolite structure.

$a$ (Å)	18.971(4)
$b$ (Å)	19.204(3)
$c$ (Å)	6.5952(12)
$\beta$ (°)	91.601(18)
$V$ (Å <sup>3</sup> )	2401.7(6)
Space group	$F1d1$
Crystal size (mm <sup>3</sup> )	0.27×0.21×0.10
$d$ (g/cm <sup>3</sup> )	2.247
Instrument	STOE STADI4
Radiation	MoK $\alpha$ = 0.71069 Å
Scan type	$\omega$ -2 $\theta$
2 $\theta$ range (°)	2.12–60.02
$h_{\min,\max}$ , $k_{\min,\max}$ , $l_{\min,\max}$	-26,26; -26,26; 0,9
$\mu$ (MoK $\alpha$ ) (mm <sup>-1</sup> )	0.773
F(000)	1631
Number of $I_{hkl}$ measured	3801
Number of unique $F_{hkl}^2$	1893
$R_{\text{int}}$	0.0397
Number of variables	236
$R$ factors for observed reflections [ $I > 2\sigma(I)$ ]	$R1 = 0.0352$ , $wR2 = 0.0743$
$R$ factors for all data	$R1 = 0.0469$ , $wR2 = 0.0794$
Residual electron density ( $e/\text{Å}^3$ )	0.486, -0.432

## Experimental

A sample of paranatrolite from Kukisvumchorr mount, Khibiny massif, Kola Peninsula, Russia, was provided by

A.P. Khomyakov. The sample was kept in a flask wrapped in moistened cotton wool. Its chemical composition was determined by X-ray fluorescence analysis (Paukov *et al.*, 2002); the amount of water was determined by thermogravimetry measurements (TG 50, Mettler TA 3000) up to 850°C. The composition corresponds to the formula Na<sub>1.88</sub>K<sub>0.22</sub>Ca<sub>0.06</sub>[Al<sub>2.24</sub>Si<sub>2.76</sub>O<sub>10</sub>] $\cdot$ 3.1H<sub>2</sub>O. To prevent dehydration, a single-crystal fragment was placed in a glass-walled capillary filled with water, and was then studied by X-ray diffraction.

Single-crystal X-ray data were collected at room temperature on a Stoe STADI-4 diffractometer (graphite-monochromatized MoK $\alpha$  radiation) using  $\omega$ -2 $\theta$  scans. The unit cell parameters were obtained from 28 independent reflections with 2 $\theta$  = 19–34°. The diffraction intensities were obtained in two steps. In the first step, the data were collected up to 2 $\theta$  = 35° for the primitive unit cell. An analysis of the systematic absences allowed us to determine the type of unit-cell centring, and in the second step, diffraction intensities were collected up to 2 $\theta$  = 60° for this centred unit cell. Experimental details for the data collection and structure determination are given in Table 1. Data reduction, including a background correction as well as Lorentz and polarization corrections, was performed with the Stoe X-RED program package. All data were empirically corrected for absorption using  $\psi$  scans. The unit cell parameters of paranatrolite are  $a$  = 6.5952(12),  $b$  = 19.204(3),  $c$  = 9.955(2) Å,  $\beta$  = 107.737(12)°, space group  $Cc$ ,  $Z$  = 4. For a convenient comparison with

Table 2. Atomic coordinates, equivalent isotropic displacement parameters  $U_{\text{eq}} = 1/3 \sum_i (\sum_j (U_{ij} a_i^* a_j^* a_i a_j))$  (Å<sup>2</sup>) and occupancies for paranatrolite.

Atom	Occupancy	$x/a$	$y/b$	$z/c$	$U_{\text{eq}}$
T1	0.59 Si/0.41 Al	0.0000	0.00342(6)	0.0000	0.0093(2)
T21	0.60 Si/0.40 Al	-0.08739(9)	0.04280(6)	0.3711(3)	0.0099(2)
T22	0.60 Si/0.40 Al	0.09389(9)	-0.04350(6)	0.3878(3)	0.0087(2)
T23	0.49 Si/0.51 Al	0.04920(9)	0.08768(6)	0.6238(3)	0.0097(2)
T24	0.47 Si/0.53 Al	-0.03967(9)	-0.08993(6)	0.6133(3)	0.0097(2)
O1	1	0.0236(2)	0.07177(17)	0.8627(6)	0.0192(7)
O10	1	-0.0190(2)	-0.06543(18)	0.8547(6)	0.0189(7)
O2	1	0.08596(18)	0.16672(17)	0.6247(6)	0.0154(7)
O20	1	-0.07726(19)	-0.16908(17)	0.6194(5)	0.0152(7)
O3	1	0.10458(17)	0.02504(18)	0.5421(6)	0.0177(7)
O30	1	-0.09452(19)	-0.03133(18)	0.5027(6)	0.0207(7)
O4	1	-0.02269(19)	0.09221(19)	0.4686(6)	0.0226(8)
O40	1	0.03522(19)	-0.09895(17)	0.4819(6)	0.0197(7)
O5	1	-0.07142(19)	0.02389(19)	0.1289(5)	0.0187(7)
O50	1	0.06725(19)	-0.01674(18)	0.1582(6)	0.0191(7)
Na1	0.973(10)	-0.02490(13)	0.21593(12)	0.4035(4)	0.0281(8)
Na10	0.977(10)	0.03054(15)	0.27995(12)	0.8792(4)	0.0319(9)
K	0.229(5)	0.1297(3)	0.3799(3)	0.3780(9)	0.0334(18)
Ow6	0.98(2)	0.0573(3)	0.1969(2)	0.1332(7)	0.0304(15)
H61	0.98	0.098(4)	0.200(4)	0.199(11)	0.032(19)*
H62	0.98	0.044(5)	0.157(5)	0.096(15)	0.06(3)*
Ow60	0.359(18)	-0.0482(10)	0.3184(7)	0.608(2)	0.048(5)
H601	0.36	-0.076(6)	0.281(5)	0.667(17)	0.00(3)*
H602	0.36	-0.064(9)	0.335(8)	0.474(15)	0.03(5)*
Ow7	0.685(15)	0.0332(4)	0.3168(3)	0.5166(13)	0.046(3)
H71	0.68	0.081(2)	0.326(4)	0.499(13)	0.003(17)*
H72	0.68	0.003(5)	0.361(5)	0.49(4)	0.13(7)*
Ow70	0.997(19)	-0.0616(3)	0.2033(3)	0.7764(10)	0.052(2)
H701	1	-0.086(8)	0.166(6)	0.704(16)	0.22(10)*
H702	1	-0.061(4)	0.197(4)	0.922(7)	0.032(19)*

\* H atoms were refined isotropically.

orthorhombic natrolite, the structure determination was carried out using *F*-centred pseudo-orthorhombic unit cell with doubled unit-cell volume (space group *F1d1*) (Table 1). The structure was solved by direct methods with the SHELXS-86 program (Sheldrick, 1986) and refined using the SHELXL-97 program (Sheldrick, 1997) with neutral atom scattering factors. Traces of Ca were ignored during the refinements. The positions, common to Ca and Na, were refined by using only the Na scattering factor. For oxygen framework positions and for extraframework positions, we followed the nomenclature of Joswig *et al.* (1984) for the scolecite structure adopting the same space group. Successive least-squares and difference Fourier analyses allowed us to determine four H atoms of the water molecules in the Ow6 and Ow70 positions due to their high occupancies. The positions of the rest of the H atoms were calculated basing on crystallochemical considerations and were added to the refined data. Except for the H61–Ow6–H62 group, all water molecules were refined with the O–H and H···H distances constrained to 1.00(5) and 1.63(5) Å, respectively. The H61 and H62 positions could be refined without restraints. Anisotropic displacement parameters for non-hydrogen atoms were used in the final stage of the refinement. The positions of the H atoms were refined isotropically. The occupation factors of the hydrogen sites were fixed as equal to the occupancies of the corresponding Ow positions. The T-position occupancy by Si and Al was estimated by the method of Mortier *et al.* (1975). Table 2 contains the coordinates, thermal parameters and occupancies for the atomic positions. The composition of parnatrolite calculated from structure data matches well with the results of the chemical analysis. Tables 3–4 list the T–O distances and the T–O–T angles, as well as the cation–H<sub>2</sub>O and the cation–O framework atom distances.

## Results and discussion

The structures of the framework compounds of the natrolite type have been described in many studies. The basic building units are fourfold rings of tetrahedra in UDUD orientation, joined by an intermediate tetra-

Table 3. T–O bond lengths (Å) and T–O–T angles (°) in parnatrolite.

T1–O1	1.663(4)		
T1–O10	1.666(4)		
T1–O5	1.667(3)		
T1–O50	1.671(4)		
mean	1.667		
T21–O2	1.650(3)	T22–O50	1.664(4)
T21–O4	1.666(4)	T22–O20	1.667(3)
T21–O5	1.674(4)	T22–O40	1.672(3)
T21–O30	1.675(4)	T22–O3	1.673(4)
mean	1.666	mean	1.669
T23–O2	1.670(3)	T24–O20	1.680(3)
T23–O4	1.684(4)	T24–O30	1.685(4)
T23–O1	1.689(4)	T24–O40	1.694(4)
T23–O3	1.695(4)	T24–O10	1.696(4)
mean	1.685	mean	1.689
T1–O1–T23	137.7(2)	T1–O10–T24	143.2(2)
T21–O2–T23	142.8(2)	T22–O20–T24	140.7(2)
T22–O3–T23	133.3(2)	T21–O30–T24	137.2(2)
T21–O4–T23	141.3(2)	T22–O40–T24	134.5(2)
T1–O5–T21	135.2(2)	T22–O50–T1	147.9(2)
		mean	139.4

dron with edge-edge orientation. The resulting [T<sub>5</sub>O<sub>10</sub>] chains build up the frameworks of fibrous zeolites having the structure types of natrolite (NAT), thomsonite (THO) and edingtonite (EDI). The frameworks of these various types differ in the mode of their chain conjunction. For the NAT-type framework, the chains are located at four levels around the 4<sub>1</sub> screw axes (Gottardi & Galli, 1985). The framework structure has the topological symmetry *I4<sub>1</sub>amd*. The actual framework is characterized by a rotation of the chains by an angle  $\psi$  (Fig. 1), which is zero only in the ideal and most symmetrical arrangement, but is 25° in natural natrolite. Alberti & Vezzalini (1981) have determined that, for natrolite, the greater the rotation angle  $\psi$ , the smaller the unit cell parameters; that is, an increase in the angle implies a compression of the structure.

Figure 1 shows a projection of the parnatrolite structure along the [001] direction. All extraframework positions are presented in the “basic” channel without regard for their statistical population. In the other channels, we show the alternative variants for the population of extraframework positions, with and without potassium.

Table 4. Na–O(Ow) and K–O(Ow) distances (Å) in parnatrolite.

<i>Na1–Ow7</i>	<b>2.341(7)</b>	Na10–Ow6	2.358(5)	K–O10	2.944(7)
Na1–O3	2.388(4)	Na10–Ow70	2.370(6)	K–O50	2.980(7)
Na1–O4	2.415(4)	<b>Na10–Ow60</b>	<b>2.413(15)</b>	K–O10	3.009(7)
Na1–Ow6	2.429(6)	Na10–O40	2.423(4)	K–O5	3.096(7)
<b>Na1–Ow60</b>	<b>2.433(15)</b>	<b>Na10–Ow7</b>	<b>2.496(9)</b>	K–O30	3.141(7)
Na1–Ow70	2.587(7)	Na10–O30	2.535(4)	K–O40	3.152(7)
Na1–O2	2.697(4)	Na10–O20	2.798(4)	K–Ow7	3.193(11)
mean	2.470	mean	2.485	mean	3.073
Na1–O20	3.044(4)	Na10–O2	2.958(4)	K–Ow60	1.699(19)
				K–Ow7	2.397(11)

Note: The pairs of alternative Na–Ow distances are given in bold italic.

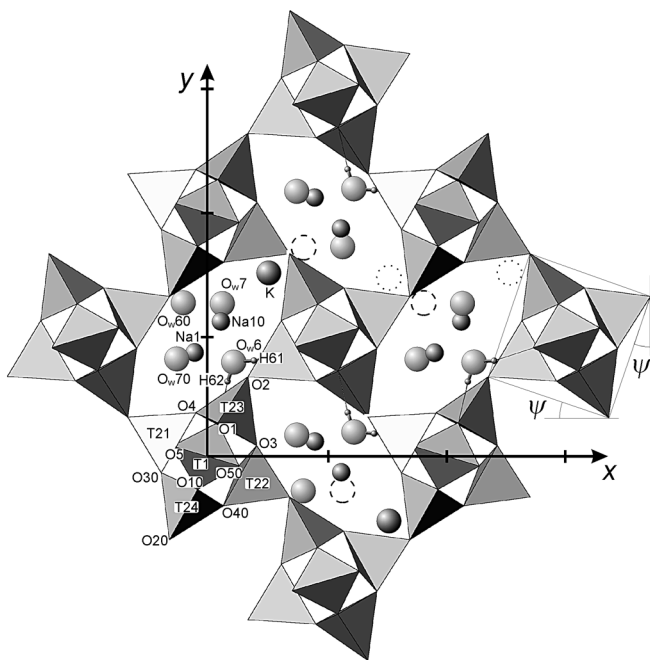


Fig. 1. A projection of the paranatrolite structure along [001]. A part of the alternative  $O_{w60}$ ,  $O_{w7}$ , and  $K$  positions are shown by broken circles. The  $\psi$  angle of the chain rotation is shown to the right.

The basic differences between the frameworks of paranatrolite and tetranatrolite are due to distinct degrees of rotation of the tetrahedral chains about the  $c$  axis. The framework of paranatrolite is more open: the  $\psi$  angle is about  $20^\circ$ , slightly smaller than  $\psi$ -values of  $22.5^\circ$  observed in tetranatrolite (Mikheeva *et al.*, 1986). The unit cell volume of paranatrolite is 4.8 % larger than that of tetranatrolite. The  $(a + b)/2$  spacing of paranatrolite is larger than  $a\sqrt{2}$  of tetranatrolite by 0.5 Å, while the  $c$  parameter is smaller by 0.04 Å.

The T–O distances range from 1.650 to 1.696 Å, and the average T–O distances for each tetrahedron cover a narrower range from 1.666 to 1.689 Å (Table 3). An estimation of the distribution of aluminum over the paranatrolite framework (Table 2) supports the conclusion of Mikheeva *et al.* (1986) that the complete disordering of Al and Si in tetranatrolite is due to the dehydration of paranatrolite. In the latter species, the differences between the Al populations of T positions do not exceed 15 %.

$Na^+$  cations are located in two positions close to those in the structures of natrolite and tetranatrolite. The coordination environment of  $Na^+$  in paranatrolite may be conveniently compared with that in natrolite, which can be considered as an archetype of the NAT group. In the natrolite structure, the  $Na^+$  cations are situated in distorted trigonal prisms  $O_4(H_2O)_2$ . Figure 2a shows the triangular bases of such prisms,  $O_{w6}-O_2-O_4$  and  $O_{20}-O_{w60}-O_3$  for  $Na1$ , and  $O_{w6}-O_2-O_{30}$  and  $O_{20}-O_{w60}-O_{40}$  for  $Na10$ . The  $O_3-O_4$  and  $O_{30}-O_{40}$  edges are significantly inclined, giving a partially unclipped twisted configuration to the prisms in the projection along their quasi-threefold axes.

The Na–O( $O_w$ ) distances range from 2.36 to 2.62 Å. In paranatrolite, the  $H_2O$  molecule ( $O_{w70}$ ) is added to the coordination sphere of  $Na^+$ . The initial coordination polyhedron is converted to a monocapped trigonal prism.  $O_{w70}$  coordinates both of the  $Na^+$  cations, being aligned in a lateral, nearly planar, prism face for  $Na10$  and an upper, very distorted, face for  $Na1$ . These tetragonal-pyramidal caps of the trigonal prisms are indicated by broken lines in Fig. 2a. In natrolite, the  $NaO_4(Ow)_2$  prisms are linked into ribbons sharing only the O– $O_w$  edges, while in paranatrolite, the  $NaO_4(Ow)_3$  polyhedra formally display common triangular  $O_{w70}-O_2-O_{w60}$  faces in addition to the common  $O_{w6}-O_{20}$  edge. However, in paranatrolite, the  $O_2-O_{20}$  distance governing the  $c$  channel aperture increases by 0.6 Å relative to the corresponding  $O_2-O_{20}$  distance in natrolite. As a result, the enlarged values of the  $Na1-O_{20}$  and  $Na10-O_2$  distances are beyond the values that should be considered for the first coordination sphere of  $Na^+$ . The monocapped prisms can be simplified to distorted  $NaO_3(Ow)_3$  octahedra. Two of these octahedra form dimers by sharing a common  $O_{w60}-O_{w70}$  edge. The dimers in turn are linked by common  $O_{w6}$  vertices and form chains running along the  $c$  axis (Fig. 2b). However, the  $O_{w60}$  position occupancy is by only 1/3. The alternative  $O_{w7}$  position (occupancy 2/3), as well as  $O_{w60}$ , coordinates both Na cations. The resulting  $NaO_3(Ow)_3$  polyhedra and the chain configurations are similar to those of the previous variant (Fig. 2c). In this way, variants should form hybrid chains along the  $c$  axis.

The  $K^+$  cations occupy positions similar to those in the structure of potassium-rich natrolite ((Meneghinello *et al.*, 1999)). The positions are situated within the eight-membered rings formed at the joins of the  $[T_5O_{10}]$  chains (Fig. 3). To an upper limit of 3.3 Å, six oxygen ligands can be found for the  $K^+$ -cations forming a very flattened distorted trigonal prism. The coordination of  $K^+$  is supplemented by the  $H_2O$  molecule of the adjacent channel *via*

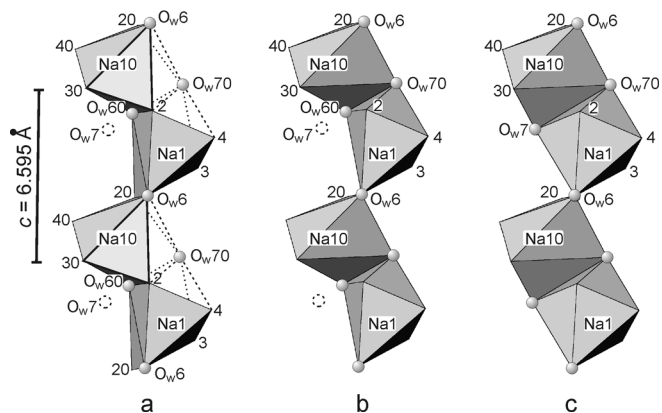


Fig. 2. Coordination polyhedra of Na cations in the paranatrolite structure. (a) Trigonal  $O_4(H_2O)_2$  prisms typical for natrolite with the extra Na– $O_{w70}$  contacts; Na–O( $O_w$ ) distances are  $< 3.1$  Å. (b) Octahedra  $O_3(H_2O)_3$ ,  $O_{w7}$  positions are vacant; Na–O( $O_w$ ) distances are  $< 2.8$  Å. (c) Octahedra  $O_3(H_2O)_3$ , the alternative possibility –  $O_{w60}$  positions are vacant.

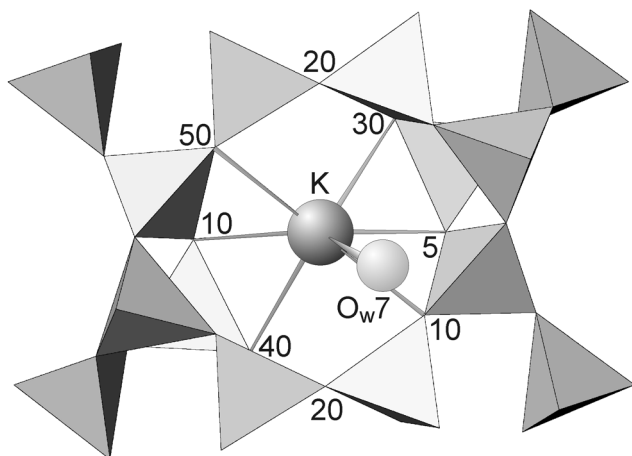


Fig. 3. Coordination environment of K in the eight-membered ring at the joint of two  $[T_5O_{10}]$  chains.

the eight-membered ring with the K–Ow7 distance of 3.193 Å.

The Ow7–K distance in the same channel is 2.4 Å, and the Ow7 position is vacant when  $K^+$  is present. In this case, the alternative Ow60 position at a distance of 1.67 Å from Ow7 is occupied, implying that the Ow60 position in the neighbouring channel (with a Ow60–K distance of 1.7 Å) must be empty. In principle, the absence of potassium in the paranatrolite structure should lead to a structure with no statistical occupation of the  $H_2O$  positions.

In the paranatrolite structure with statistical (Al,Si)-ordering, we may expect the disordering of hydrogen bonds. Table 5 lists the Ow–O and Ow–Ow distances, as well as the probable hydrogen bonds between  $H_2O$

molecules and the framework oxygen atoms. The Ow6 environment coincides partially with that of the  $H_2O$  position in the natrolite structure. There are two short Ow6–O distances, while all the others exceed 3.3 Å. The refined H atoms at the Ow6 position with an H–Ow–H angle of  $118(8)^\circ$  form the hydrogen bonds with O1 and O5. For the other  $H_2O$  positions with Ow–O distances in the range  $< 3.3$  Å, the refinement of the H positions does not allow an unambiguous selection of the ligands (Table 5). We believe that this is due to the aluminum disorder in the paranatrolite framework and hence the orientation disordering of the H vectors of the  $H_2O$  molecules.

As mentioned above, paranatrolite converts into tetranatrolite upon partial dehydration. Mikheeva *et al.* (1986) studied potassium-rich and calcium-poor tetranatrolite from Khibiny, using material developed from paranatrolite. The composition of tetranatrolite was arbitrarily taken as equal to that of the paranatrolite (Khomyakov *et al.*, 1986) with a 1/3 reduction in the amount of water. The potassium positions were not located in the tetranatrolite crystal structure. Furthermore, Mikheeva *et al.* (1986) did not take into account of the excess water that was recorded during thermogravimetric analysis. However, the additional water positions were located in the crystal structure of calcium-rich potassium-poor tetranatrolite (Mazzi *et al.*, 1986; Evans *et al.*, 2000). In our opinion, the data on the crystal structure of Khibiny tetranatrolite need to be re-investigated; we point out that such work is in progress. After revising the structure, we should then be able to analyse the mechanism of the paranatrolite–tetranatrolite transition in detail.

**Acknowledgements:** Authors are indebted to Dr A.P. Khomyakov for providing the paranatrolite sample. Many

Table 5. Selected surroundings of  $H_2O$  molecules and determined H bond lengths (Å) and angles ( $^\circ$ ) in paranatrolite.

Ow...O	$d_{Ow...O}$		Ow...O	$d_{Ow...O}$
Ow6...O5	2.833(6)		Ow7...O10	2.679(7)
Ow6...O1	3.050(6)		Ow7...O30	2.840(8)
			Ow7...O2	3.127(7)
Ow60...O10	2.852(15)		Ow7...Ow60	1.67(2)
Ow60...O20	3.264(15)			
Ow60...O3	3.279(15)		Ow70...O50	2.763(6)
Ow60...O40	3.299(14)		Ow70...O1	3.043(7)
Ow60...Ow70	2.489(15)		Ow70...O4	3.050(6)
Ow60...Ow7	1.67(2)		Ow70...O2	3.080(6)
			Ow70...Ow60	2.489(15)
Ow–H...O	$d_{Ow-H}$	$d_{H...O}$	$d_{Ow...O}$	$\angle Ow-H...O$
Ow6–H61...O5	0.88(8)	1.97(8)	2.833(6)	166(6)
Ow6–H62...O1	0.84(10)	2.27(10)	3.050(6)	154(9)
Ow60–H602...O10	0.98(5)	2.25(12)	2.851(15)	119(10)
Ow60–H602...O20	0.98(5)	2.34(9)	3.264(15)	156(16)
Ow7–H71...O30	0.93(4)	2.33(7)	2.840(8)	114(6)
Ow7–H72...O10	1.03(5)	1.71(11)	2.679(7)	154(17)
Ow70–H701...O4	0.98(5)	2.44(13)	3.050(6)	120(11)
Ow70–H702...O50	0.97(4)	2.66(7)	2.763(6)	85(4)

thanks to associate editor Dr. V. Kahlenberg and two anonymous reviewers, who helped up to improve the manuscript. This work was supported by the Russian Foundation for Basic Research (grant # 01-05-65414) and the U.S. Civilian Research & Development Foundation for the Independent States of the Former Soviet Union (CRDF, grant # REC-008).

## References

- Alberti, A. & Vezzalini, G. (1981): A distorted natrolite: relationship between cell parameters and Si-Al distribution. *Acta Cryst.*, **B37**, 781-788.
- , — (1983): How the structure of natrolite is modified through the heating-induced dehydration. *N. Jb. Miner. Mh.*, **3**, 135-144.
- Baur, W.H. (1991): Concerning the crystal structure refinement of paranatrolite published by F. Pechar. *Cryst. Res. Technol.*, **26**, K 169-K 171.
- Belitsky, I.A., Fursenko, B.A., Gabuda, S.P., Kholdeev, O.V., Seryotkin, Yu.V. (1992): Structural transformations in natrolite and edingtonite. *Phys. Chem. Minerals*, **18**, 497-505.
- Chao, G.Y. (1980): Paranatrolite, a new zeolite from Mont St-Hillaire, Québec. *Can. Mineral.*, **18**, 85-88.
- Coombs, D.S., Alberti, A., Armbruster, T., Artioli, G., Colella, C., Galli, E., Grice, J.D., Liebau, F., Mandarino, J.A., Minato, H., Nickel, E.H., Passaglia, E., Peacor, D.R., Quartieri, S., Rinaldi, R., Ross, M., Sheppard, R.A., Tillmans, E., Vezzalini, G. (1997): Recommended nomenclature for zeolite minerals: Report of the subcommittee on zeolites of the International Mineralogical Association, Commission on New Minerals and Mineral Names. *Can. Mineral.*, **35**, 1571-1606.
- Evans, H.T.Jr., Konnert, J.A., Ross, M. (2000): The crystal structure of tetranatrolite from Mont Saint-Hillaire, Québec, and its chemical and structural relationship to paranatrolite and gonnardite. *Am. Mineral.*, **85**, 1808-1815.
- Joswig, W., Bartl, H., Fuess, H. (1984): Structure refinement of scolecite by neutron diffraction. *Z. Kristallogr.*, **166**, 219-223.
- Khomyakov, A.P., Cherepivskaya, G.E., Mikheeva, M.G. (1986): The first occurrence of paranatrolite in the USSR. *Dokl. Akad. Nauk SSSR*, **288**, 214-217.
- Mazzi, F., Larsen, A.O., Gottardi, G., Galli, E. (1986): Gonnardite has the tetrahedral framework of natrolite: experimental proof with a sample from Norway. *N. Jb. Miner. Mh.*, **5**, 219-228.
- Meneghinello, E., Martucci, A., Alberti, A., Di Renzo, F. (1999): Structural refinement of a K-rich natrolite: evidence of a new extraframework cation site. *Micropor. Mesopor. Mater.*, **30**, 89-94.
- Mikheeva, M.G., Pushcharovskii, D.Yu., Khomyakov, A.P., Yamnova, N.A. (1986): Crystal structure of tetranatrolite. *Soviet Phys. Crystallogr. (Eng. ed.)*, **31**, 254-257.
- Mortier, W.J., Pluth, J.J., Smith, J.V. (1975): Positions of cations and molecules in zeolites with the mordenite-type framework. II. Dehydrated hydrogen-ptilolite. *Mater. Res. Bull.*, **10**, 1317-1326.
- Paukov, I.E., Belitskii, I.A., Kovalevskaya, Yu.A. (2002): Heat capacity of paranatrolite at low temperatures. *Geochem. Int.*, **40**, 823-826.
- Pechar, F. (1988): Structure refinement of paranatrolite by X-ray diffraction. *Cryst. Res. Technol.*, **23**, 647-653.
- Sheldrick, G.M. (1986): SHELXS-86. Program for solving crystal structures. Univ. Göttingen, Germany.
- (1997): SHELXL-97. Program for refinement of crystal structures. Univ. Göttingen, Germany.

Received 14 January 2003

Modified version received 22 July 2003

Accepted 16 December 2003